e-ISSN 2083–4640
ISSN 1507–1367

CASE REPORT

Reports of Practical Oncology and Radiotherapy
2021, Volume 26, Number 3, pages: 470–474
DOI: 10.5603/RPOR.a2021.0052
Submitted: 19.09.2021
Accepted: 23.02.2021

Superparamagnetic iron oxide-enhanced MRI-guided stereotactic ablative radiation therapy for liver metastasis

Yukihiro Hama, Etsuko Tate

Department of Radiation Oncology, Tokyo-Edogawa Cancer Centre, Edogawa Hospital, Tokyo, Japan

ABSTRACT

Background: MRI-guided radiation therapy can image a target and irradiate it at the same time. Superparamagnetic iron oxide (SPIO) is a liver-specific contrast agent that can selectively visualize liver tumors, even if plain MRI does not depict them. The purpose of this study was to present a proof of concept of SPIO-enhanced MRI-guided radiation therapy for liver tumor.

Case presentation: MRI-guided stereotactic ablative radiation therapy (SABR) was planned for a patient with impaired renal function who developed liver metastases after nephroureterectomy for ureteral cancer. Because liver metastasis was not visualized on plain MRI, SPIO-enhanced MRI was performed at 0.35 T using true fast imaging with steady-state free precession (true FISP) pulse sequence and SABR was performed. Liver metastasis was clearly visualized by SPIO-enhanced MRI, and MRI-guided SABR was performed without adverse events.

Conclusion: Even if liver metastasis is not visualized by plain MRI, liver metastasis can be clearly depicted by administering SPIO, and MRI-guided radiation therapy can be performed.

Key words: image-guided radiation therapy; stereotactic radiation therapy; contrast media; magnetic resonance imaging; steady-state free precession MRI

Rep Pract Oncol Radiother 2021;26(3):470–474

Introduction

In patients with recurrent and/or metastatic urothelial carcinoma of the ureter, combination chemotherapy yields high response rates but the prognosis is poor [1]. Patients with a prior history of bladder cancer have been shown to have even worse disease-free survival rates [2]. Stereotactic ablative radiation therapy (SABR) has been suggested to improve the prognosis of patients with oligometastases defined by both number (typically, less than 5) and location [3, 4]. When SABR is applied to liver metastasis, it is necessary to set a large margin because liver metastasis moves greatly by breathing. MRI-guided radiation therapy can track the movement of the tumor and surrounding normal tissues, which allows a higher dose of radiation to be administered to the tumor while minimizing the amount of radiation delivered to the normal tissues [5, 6]. One of the drawbacks of MRI-guided radiation therapy is the poor visibility of a liver tumor during irradiation. Since the contrast enhancement by extracellular gadolinium-based contrast agents (GBCAs) is transient, sustained tumor visualization is not possible. Gadoxetate disodium, a hepatocyte-specific linear GBCA, may allow for sustained tumor visualization, but linear GBCAs result in more retention and retention for a longer time than macrocyclic GBCAs. Therefore, gadoxetate cannot be used in patients with poor renal

Address for correspondence: Yukihiro Hama, M.D., Ph.D., Department of Radiation Oncology, Tokyo-Edogawa Cancer Centre, Edogawa Hospital, 2–24–18 Higashikoiwa, Edogawa, Tokyo, 133–0052, Japan, tel: +81-3-3673-1221; e-mail: yjhama2005@yahoo.co.jp

function due to the risk of nephrogenic systemic fibrosis (NSF). To overcome these limitations, we used liver-specific superparamagnetic iron oxide (SPIO), and performed MRI-guided SABR for a solitary liver metastasis from the ureteral carcinoma. As far as we know, this is the first report of MRI-guided SABR for liver metastasis using SPIO.

Case presentation

A 74-year-old man with a solitary liver metastasis from urothelial carcinoma of the ureter was referred to our hospital for radiation therapy. He had undergone a nephroureterectomy with bladder cuff excision for localized ureteral cancer (Stage II, urothelial carcinoma, Grade 1) four and a half years ago. He also had a history of early-stage bladder cancer 13 years previously, but it was cured by transurethral resection. The patient had no subjective symptoms at the time of referral, but whole-body CT showed a solitary liver metastasis. The patient was initially recommended for combination chemotherapy but refused, so he was treated with MRI-guided SABR after the protocol was approved by the institutional review board and the written informed consent was obtained from the patient.

SPIO-induced signal changes at 0.35T

Prior to the radiotherapy treatment planning, anatomical shape and cancer cell viability of the tumor were evaluated by multiparametric MRI at 3T (MAGNETOM Skyra, Siemens Healthcare, Erlangen, Germany). The liver metastasis was hyperintense relative to adjacent liver parenchyma on breath-hold half-Fourier-acquired single-shot turbo spin echo (HASTE) imaging (Fig. 1A), and

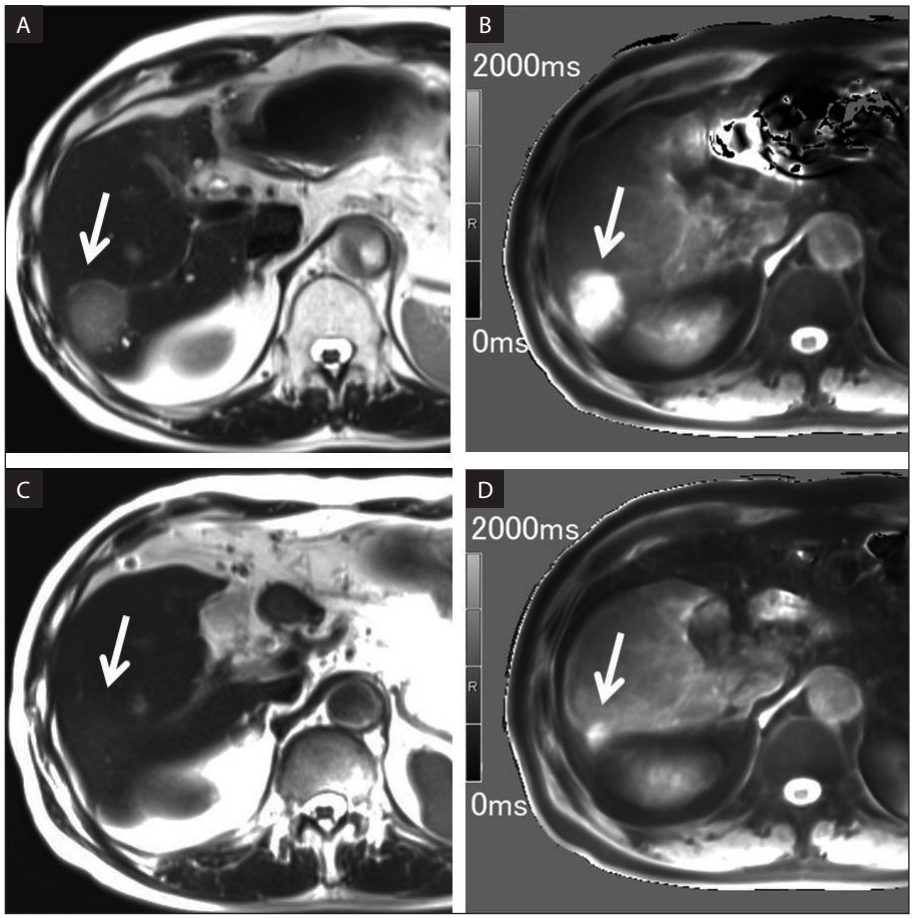

Figure 1. Multiparametric MRI at 3T before and 3 months after treatment. The liver metastasis (arrow) was hyperintense relative to adjacent liver parenchyma on HASTE imaging (TR/TE/FA = 1100 ms/95 ms/160 degree) **(A)**; T1 times of the tumor (arrow) were shorter than those of adjacent liver parenchyma on quantitative T1 mapping **(B)**; Three months after MRI-guided SABR, the tumor volume reduced significantly on HASTE imaging (arrow) **(C)**; Quantitative T1 map imaging (arrow) (**D**). HASTE — half-flourier-acquired single-shot turbo spin echo; TR — repetition time; TE — echo time; FA — flip angle; SABR — stereotactic ablative radiation therapy

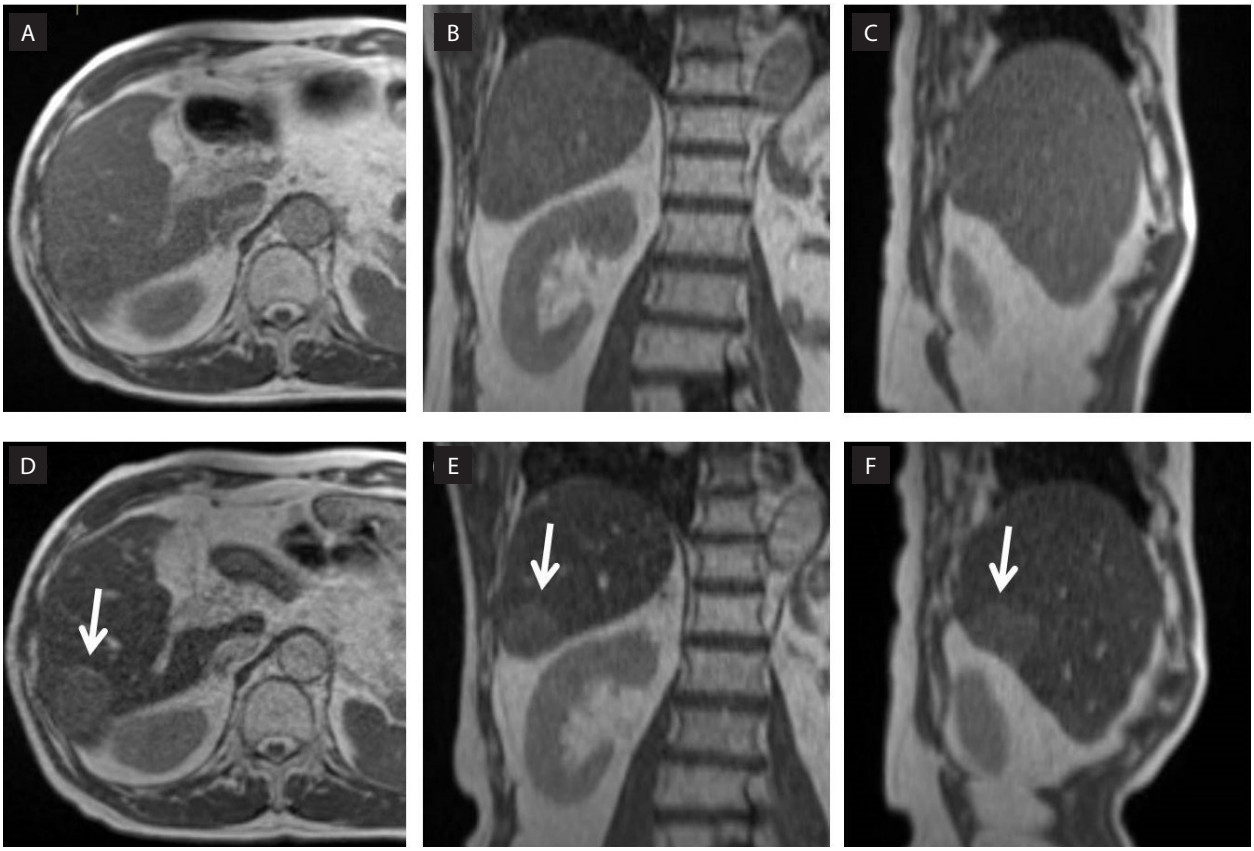

Figure 2. Plain and SPIO-enhanced true FISP images at 0.35T. Liver metastasis is barely visible on non-contrast enhanced true FISP images consisting of axial (**A**), coronal (**B**) and sagittal (**C**) planes. After SPIO administration, liver metastasis (arrows) is clearly visualized on true FISP images consisting of axial (**D**), coronal (**E**) and sagittal (**F**) planes; SPIO — superparamagnetic iron oxide; FISP — fast imaging with steady-state free precession

T1 times of the tumor were substantially shorter than those of adjacent liver parenchyma on quantitative T1 mapping (qT1) reflecting cancer cell viability (Fig. 1B). Then, the patient underwent MRI simulation on 0.35T MRI-guided radiotherapy system (MRIdian® System, ViewRayTM Inc, Oakwood Village, Ohio, USA) with surface coils on the abdomen using true fast imaging with steady-state free precession (true FISP) images (3.33 ms TR, 1.43 ms TE, 60 flip angle, 3 mm slice thickness, 40 cm × 40 cm × 43 cm field of view) (Fig. 2A–C). Patients were simulated at shallow breathing. At MRI simulation, tumor motion was evaluated using real-time cine MRI in the sagittal plane and the patient's ability to breath-hold evaluated for reproducibility and tolerance. But the tumor could not be clearly visualized by true FISP imaging with a 0.35T MRI unit that would be imaged during irradiation. Since the image contrast with True FISP is determined by T2/T1 or T2*/T1 properties, a hepatocyte-specific contrast agent, ferucarbotran (Resovist, Bayer Healthcare) was injected intravenously. Ferucarbotran is the clinically approved SPIO which causes marked shortening in T2 relaxation time resulting in a loss of signal in the liver. One hour after the administration of ferucarbotran, the lesion of liver metastasis was clearly visualized on true FISP image (Fig. 2D–F).

Radiation therapy planning using SPIO-enhanced MRI

Fusion images of post-contrast true FISP imaging at 0.35T and multiparametric MRI at 3T were generated using Monaco 5.0 treatment planning software (Elekta AB, Stockholm, Sweden), and gross tumor volume (GTV) was defined by one radiologist and one radiation oncologist. Planning target volume (PTV) was defined as a 1 mm margin expansion from GTV. The prescribed dose to the D95% of the PTV (the dose covering 95% of the PTV) was 40 Gy in 5 fractions over 5 days (Fig. 3A–C). Treatment plan was carried out us-

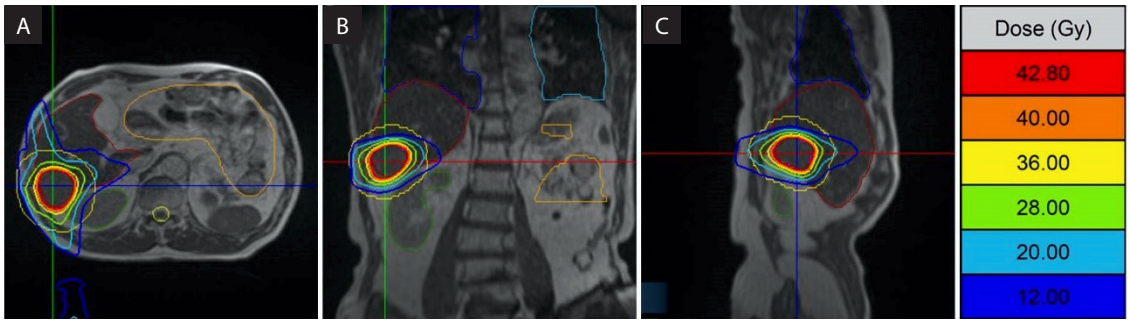

Figure 3. MRI-guided SABR isodose line distribution. Isodose lines are displayed on axial (**A**), coronal (**B**), and sagittal (**C**) true FISP images. Isodose lines with corresponding actual radiation dose were given over 5 fractions. SABR — stereotactic ablative radiation therapy; FISP — fast imaging with steady-state free precession

ing intensity-modulated radiation therapy (IMRT) and the maximum dose within PTV was not constrained. The daily treatment MRI was aligned to the simulation MRI to ensure appropriate tumor position. During treatment delivery, a sagittal True FISP sequence (2.1 ms TR, 0.91 ms TE, 60 flip angle, 7 mm slice thickness, 35 cm × 35 cm field of view, 4 frames per second) was acquired.

Results

MRI-guided SABR was performed on the MRI-guided radiation therapy unit using a 0.35T magnet, Co-60 delivery, and real-time MRI acquisition. Since the contrast effect of SPIO was sustained during the treatment period, no additional ferucarbotran was given. There were no radiation-induced adverse events during treatment and three months of follow-up. Three months later, the tumor volume reduced significantly on both HASTE and qT1 images.

Discussion

MRI-guided radiotherapy can monitor the movement of the tumor and the surrounding organs at risk in real time and reduce radiation-induced adverse effects by reducing the amount of radiation exposure to surrounding normal tissues. In order to monitor the tumor movement in real time, it is necessary to use a fast repeating imaging pulse sequence. The true FISP sequence is a fast imaging technique with a high signal-to-noise ratio (SNR), and for most true FISP imaging a bright T2/T1 signal is desired. Since the lesion was hyperintense on HASTE imaging taken with a 3T MRI unit and the image contrast with true FISP is determined by T2/T1 or T2*/T1 properties, we hypothesized that the T2 shortening effect of SPIO would reduce the signal intensity of the surrounding liver parenchyma and keep the tumor signal hyperintense.

There has been a case report that the liver tumor was visualized using gadoxetate during real-time MRI-guided radiation therapy of the liver [**6**]. However, we thought it was more appropriate for this patient to be administered ferucarbotran instead of gadoxetate for the following three reasons. First, the patient's left kidney was resected and his renal function was poor. Given the risk of linear GBCAs including gadoxetate, we thought that there was no rational basis to administer gadoxetate [7, 8]. On the other hand, there are reports with 0.026% side effect while using gadoxetate as a contrast agent, with no increased incidence of side effects noted in impaired renal or hepatic function. Furthermore, due to dual renal and hepatic excretion, there are no reported cases of nephrogenic toxic fibrosis in some series [9, 10]. Further research is needed to determine which one is the more suitable contrast agent. Second, since the tissue contrast of true FISP images is determined by the T2/T1 or T2*/T1 properties, T2 shortening effects or spin-spin interactions caused by SPIO have a greater impact on signal intensity than gadoxetate. Third, since the contrast enhancement of ferucarbotran persists for about 4 days after administration [11], it is not necessary to additionally administer ferucarbotran at every treatment session.

The limitation of this study is that the pulse sequence used in MRI-guided radiotherapy is not optimized. R1, R2 and R2* relaxation rates of liver

parenchyma and tumor should have been measured before and after SPIO administration using 0.35T MRI unit. Furthermore, since the spin-spin interaction at 1.5T is larger than that at 0.35T, the contrast between the tumor and the liver might be greater using a high-field 1.5T MRI unit. Third, gadoxetate is the standard contrast agent used for imaging liver metastasis or primary liver tumors. On the other hand, SPIO is available in limited countries, and its worldwide use is not established [12].

Conclusions

A single case study cannot be generalized to others without further scientific verifications; however, if liver tumors are not visualized by plain MRI, administration of SPIO may be a solution for MRI-guided radiation therapy.

Conflict of interest

None declared.

Funding

None declared.

Acknowledgements

None declared.

Authors' contributions

Study concept, design, definition of intellectual content, literature search, clinical studies, data acquisition, data analysis, manuscript preparation, editing and review — Y.H., E.T; statistical analysis — N/A; experimental studies — N/A.

References

1. Loehrer PJ, Einhorn LH, Elson PJ, et al. A randomized comparison of cisplatin alone or in combination with methotrexate, vinblastine, and doxorubicin in patients with metastatic urothelial carcinoma: a cooperative group study. J Clin Oncol. 1992; 10(7): 1066–1073, doi: 10.1200/jco.1992.10.7.1066, indexed in Pubmed: 1607913 .
2. Mullerad M, Russo P, Golijanin D, et al. Bladder cancer as a prognostic factor for upper tract transitional cell carcinoma. J Urol. 2004; 172(6 Pt 1): 2177–2181, doi: 10.1097/01.ju.0000144505.40915.98, indexed in Pubmed: 15538226.
3. Onderdonk BE, Gutiontov SI, Chmura SJ. The Evolution (and Future) of Stereotactic Body Radiotherapy in the Treatment of Oligometastatic Disease. Hematol Oncol Clin North Am. 2020; 34(1): 307–320, doi: 10.1016/j.hoc.2019.09.003, indexed in Pubmed: 31739951.
4. Lievens Y, Guckenberger M, Gomez D, et al. Defining oligometastatic disease from a radiation oncology perspective: An ESTRO-ASTRO consensus document. Radiother Oncol. 2020; 148: 157–166, doi: 10.1016/j.radonc.2020.04.003, indexed in Pubmed: 32388150.
5. van de Lindt TN, Fast MF, van Kranen SR, et al. MRI-guided mid-position liver radiotherapy: Validation of image processing and registration steps. Radiother Oncol. 2019; 138: 132–140, doi: 10.1016/j.radonc.2019.06.007, indexed in Pubmed: 31252295.
6. Wojcieszynski AP, Rosenberg SA, Brower JV, et al. Gadoxetate for direct tumor therapy and tracking with real-time MRI-guided stereotactic body radiation therapy of the liver. Radiother Oncol. 2016; 118(2): 416–418, doi: 10.1016/j.radonc.2015.10.024, indexed in Pubmed: 26627702.
7. Erdoğan MA, Apaydin M, Armagan G, et al. Evaluation of toxicity of gadolinium-based contrast agents on neuronal cells. Acta Radiol. 2021; 62(2): 206–214, doi: 10.1177/0284185120920801, indexed in Pubmed: 32366109.
8. Chehabeddine L, Al Saleh T, Baalbaki M, et al. Cumulative administrations of gadolinium-based contrast agents: risks of accumulation and toxicity of linear vs macrocyclic agents. Crit Rev Toxicol. 2019; 49(3): 262–279, doi: 10.1080/10408444.2019.1592109, indexed in Pubmed: 30942117.
9. Endrikat JS, Dohanish S, Balzer T, et al. Safety of gadoxetate disodium: Results from the clinical phase II-III development program and postmarketing surveillance. J Magn Reson Imaging. 2015; 42(3): 634–643, doi: 10.1002/jmri.24838, indexed in Pubmed: 25643844.
10. Lauenstein T, Ramirez-Garrido F, Kim YH, et al. Nephrogenic systemic fibrosis risk after liver magnetic resonance imaging with gadoxetate disodium in patients with moderate to severe renal impairment: results of a prospective, open-label, multicenter study. Invest Radiol. 2015; 50(6): 416–422, doi: 10.1097/RLI.0000000000000145, indexed in Pubmed: 25756684.
11. Reimer P, Balzer T. Ferucarbotran (Resovist): a new clinically approved RES-specific contrast agent for contrast-enhanced MRI of the liver: properties, clinical development, and applications. Eur Radiol. 2003; 13(6): 1266–1276, doi: 10.1007/s00330-002-1721-7, indexed in Pubmed: 12764641.
12. Wang YXJ. Current status of superparamagnetic iron oxide contrast agents for liver magnetic resonance imaging. World J Gastroenterol. 2015; 21(47): 13400–13402, doi: 10.3748/wjg.v21.i47.13400, indexed in Pubmed: 26715826.